Accepted Manuscript

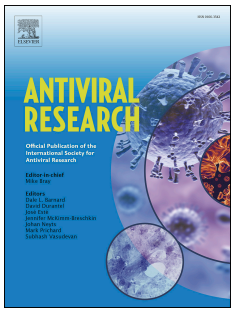

Significant inhibition of re-emerged and emerging swine enteric coronavirus *in vitro* using the multiple shRNA expression vector

Kai Li, Hao Li, Zhen Bi, Deping Song, Fanfan Zhang, Dan Lei, Suxian Luo, Zhiquan Li, Wang Gong, Dongyan Huang, Yu Ye, Yuxin Tang

PII: S0166-3542(18)30622-3

DOI: https://doi.org/10.1016/j.antiviral.2019.03.010

Reference: AVR 4492

To appear in: *Antiviral Research*

Received Date: 15 October 2018

Revised Date: 13 March 2019

Accepted Date: 18 March 2019

Please cite this article as: Li, K., Li, H., Bi, Z., Song, D., Zhang, F., Lei, D., Luo, S., Li, Z., Gong, W., Huang, D., Ye, Y., Tang, Y., Significant inhibition of re-emerged and emerging swine enteric coronavirus *in vitro* using the multiple shRNA expression vector, *Antiviral Research* (2019), doi: https://doi.org/10.1016/j.antiviral.2019.03.010.

Significant inhibition of re-emerged and emerging swine enteric coronavirus *in vitro* using the multiple shRNA expression vector

Kai Li[1, 2 #], Hao Li[1, 2 #], Zhen Bi[1, 2], Deping Song[1, 2], Fanfan Zhang[1, 2], Dan Lei[1, 2], Suxian Luo[1, 2], Zhiquan Li [1, 2], Wang Gong[1, 2], Dongyan Huang[1, 2], Yu Ye[1, 2 *], Yuxin Tang[1, 2 *]

[1] Department of Preventive Veterinary Medicine, College of Animal Science and Technology, Jiangxi Agricultural University, Nanchang, Jiangxi, 330045, China

[2] Key Laboratory for Animal Health of Jiangxi Province, Nanchang, Jiangxi, 330045, China.

[#] These authors contributed equally to this work.

[*] Correspondence: YY: yy6157832@163.com; YT: tang53ster@gmail.com.

ABSTRACT

Swine enteric coronaviruses (SECoVs), including porcine epidemic diarrhea virus (PEDV), swine acute diarrhea syndrome coronavirus (SADS-CoV), and porcine deltacoronavirus (PDCoV) have emerged and been prevalent in pig populations in China for the last several years. However, current traditional inactivated and attenuated PEDV vaccines are of limited efficacy against circulating PEDV variants, and there are no commercial vaccines for prevention of PDCoV and SADS-CoV. RNA interference (RNAi) is a powerful tool in therapeutic applications to inhibit viral replication *in vitro*. In this study, we developed a small interfering RNA generation system that expressed two different short hairpin RNAs (shRNAs) targeting the M gene of PEDV and SADS-CoV and the N gene of PDCoV, respectively. Our results demonstrated that simultaneous expression of these specific shRNA molecules inhibited expression of PEDV M gene, SADS-CoV M gene, and PDCoV N gene RNA by 99.7%, 99.4%, and 98.8%, respectively, in infected cell cultures. In addition, shRNA molecules significantly restricted the expression of M and N protein, and impaired the replication of PEDV, SADS-CoV, and PDCoV simultaneously. Taken together, this shRNAs expression system not only is proved to be a novel approach for studying functions of various genes synchronously, but also developed to test aspects of a potential therapeutic option for treatment and prevention of multiple SECoV infections.

Keywords: multiple short hairpin RNAs; swine enteric coronavirus; multi-resistance strategy

INTRODUCTION

Swine enteric coronaviruses (SECoVs), including porcine epidemic diarrhea virus (PEDV) and porcine deltacoronavirus (PDCoV), have emerged and spread throughout the swine industry in China in recent years (Dong et al., 2016; Li et al., 2012; Song et al., 2015). Swine acute diarrhea syndrome coronavirus (SADS-CoV) is a novel coronavirus which was first reported in southern China in 2017. It also can cause severe diarrhea disease in newborn piglets (Fu et al., 2018; Gong et al., 2017; Pan et al., 2017; Wang et al., 2018a; Wang et al., 2018b; Xu et al., 2018; Zhou et al., 2018a; Zhou et al., 2018b). Similar to other SECoVs, such as transmissible gastroenteritis virus (TGEV), these re-emerged and emerging SECoV diseases are age-dependent with high morbidity and mortality in neonatal pigs. Mixed infections of PEDV, SADS-CoV, and PDCoV are presented in swine herds, which mostly are double infections or successive infections (Ajayi et al., 2018; Niederwerder and Hesse, 2018; Trudeau et al., 2017; Zhou et al., 2018b). Currently, vaccination is the primary measure for prevention of PEDV. However, genetic variants of PEDV have been identified in Asia, Europe, and North America since 2010 (Bevins et al., 2018; Guo et al., 2018; Su et al., 2018; Yu et al., 2018). Traditional inactivated and attenuated PEDV vaccines failed to provide robust protection against PEDV variants infection (Lee et al., 2018; Li et al., 2018b; Li et al., 2017; Park and Shin, 2018). Meanwhile, SADS-CoV and PDCoV have no commercial vaccines yet (Fu et al., 2018; Hu et al., 2015; Ma et al., 2015). Therefore, given complexity of mixed viral infection and issues associated with novel antigenic variants, novel antiviral strategies may provide means of effectively addressing issues of SECoV infection in swine.

RNA interference (RNAi) is a process in which the gene expression can be silenced in a sequence-specific manner mediated by shRNA, making it a powerful approach in therapeutic

applications (Berkhout, 2018). In recent years, RNAi has been successfully developed as a new antiviral therapy regimen, and widely used to inhibit viral replication *in vitro* and *in vivo*, including against human immunodeficiency virus type 1 (HIV-1) (Lau et al., 2007), severe acute respiratory syndrome coronavirus (Li et al., 2005), influenza virus (Sui et al., 2009), classical swine fever virus (Li et al., 2011), foot-and-mouth disease virus (Oh et al., 2018) and TGEV (Zhou et al., 2010). A plasmid-transcribed shRNA against PEDV has been reported (Shen et al., 2015). However, the single-shRNA expression vector has several limitations in protecting from SECoVs infection, especially under the complex co-infection of multiple viruses or different genotypes. Previous studies showed that after long-term culturing, some viruses including HIV and hepatitis C virus could evolve to escape recognition of RNAi machinery by accumulating point mutations that change the target site of sequence directly or the local secondary structure nearby (Lau et al., 2007; Watanabe et al., 2014). An alternative approach for preventing this emergence of escape mutants is the simultaneous use of multiple shRNAs (Pulloor et al., 2014). Against hepatitis B virus (HBV), a plasmid encoding three shRNAs driven by a single RNA polymerase III promoter U6 was more effective in limiting viral infection than single shRNA (Chen and Mahato, 2008). In coronavirus, membrane (M) and nucleocapsid (N) genes are highly conserved among genotypes and have pivotal roles in the viral life cycle (Kuo et al., 2016; Mason et al., 2003; Stadejek et al., 2013), thus making them candidates for the design of antiviral RNAi.

For the development of a durable gene therapy that blocks the replication of multiple SECoVs simultaneously, different shRNAs targeting PEDV (CH/JXJA/2017, accession no. **MF375374.1**) (Li et al., 2018a), SADS-CoV (CH/FJWT/2018, accession no. **MH615810.1**), and PDCoV (CH/JXNI/02/2015, accession no. **KR131621.1**) (Song et al., 2015) were independently

screened, then a single plasmid expressing multiple shRNA (multi-shRNA) against these viruses was constructed. This multi-shRNA expression system was capable of protecting against viral infection *in vitro* by silencing the sequences of PEDV, SADS-CoV, and PDCoV. Our results highlighted the feasibility of RNAi-based technology as a potential therapy against multiple SECoVs.

MATERIALS AND METHODS

Cell culture, virus propagation

Both Vero-81 cells and LLC-PK1 cells were maintained in DMEM (GIBCO, USA) supplemented with 10% fetal bovine serum (FBS) at 37°C in a humidified atmosphere with 5% CO_2. These SECoVs (CH/JXJA/2017, CH/FJWT/2018, and CH/JXNI/02/2015) were isolated from sick piglets with typical symptoms of diarrhea and propagated in Vero-81 cells or LLC-PK1 cells as previously described and stored in our lab (Li et al., 2018a; Song et al., 2015; Zhou et al., 2018b).

SiRNAs sequences selection and multiple shRNAs expression plasmid construction

Two siRNA sequences for the inhibition of CH/JXJA/2017, CH/FJWT/2018, and CH/JXNI/02/2015 were designed by Block-iT™ RNAi Designer program (http://rnaidesigner.thermofisher.com/rnaiexpress/), and a BLAST search (http://www.ncbi.nlm.nih.gov/BLAST) was performed to remove all possible homologous sequences (Supplementary Table 1). Next, an shRNA expression plasmid was constructed through a series of cloning steps (Supplementary Figure 1). Using pSpCas9(BB)-2A-mCherry as a donor, *Mlu*□ and *Bgl*□ restriction endonuclease sites were added upstream and downstream, respectively,

the human U6 small nuclear promoter (hU6) sequence. Meanwhile, *Hind*□ and *Xba*□ restriction endonuclease sites were linked to both ends, separately, of the mCherry fluorescent protein reporter sequence gene using PCR amplification. Afterward, a second U6 promoter construct was flanked *Bgl*□-*Eco*R□ and *Xho*□-*Kpn*□-*Bam*H□ restriction endonuclease sequences by PCR, respectively. This second U6 promoter was cloned using *Bgl*□ / *Bam*H□ into the *Bgl*□ site of to generate the multi-shRNA expression construct pSil-Double-U6-mCherry (Supplementary Figure 1). The fragment of shRNA targeting PEDV and SADS-CoV M gene, which is identical between PEDV and SADS-CoV (Supplementary Table 1), was digested by *Bgl*□ and *Eco*R□, and the fragment of shRNA targeting PDCoV N gene was digested by *Xho*□ and *Kpn*□ and then were successively cloned into pSil-Double-U6-mCherry to yield pMulti-shRNA-M/N-mCherry (Table 1). A shRNA vector pSil-shRNA-NC-mCherry targeting a non-specific sequence was generated as a nonspecific transfection control. The plasmids constructed above were validated by PCR identification and DNA sequencing.

Generation of Vero-81 or LLC-PK cells with stable expression of multiple-shRNA and virus infection

Vero-81 or LLC-PK1 cells were seeded (2.5×10^4/well) into 6-well plates. When cells reached 80-90% confluence, cells were transfected with 2.5 μg/well of pMulti-shRNA-M/N-mCherry and pSil-shRNA-NC-mCherry using the Lipofectamine^{TM} 2000 Transfection Reagent (Thermo Fisher, USA). After incubating for 24 h, the medium was replaced with 2% FBS containing 1000 μg/ml of Neomycin (G418). These resistant cell clones were maintained in G418-containing media for 15 days with routine medium replacements until cell death could no longer be observed. Then, these Vero-81 or LLC-PK1 monoclonal cells transfected with pMulti-shRNA-M/N-mCherry and

pSil-shRNA-NC-mCherry were sreened by limiting dilution analysis (LDA) as described previously (Oh et al., 2018), and cultured in media with addition of G418 (500 μg/ml) in 6-well plates at 37°C in a 5% CO_2 atmosphere. After reaching 90-100% confluence, these plasmid-transduced Vero-81 or LLC-PK1 cells were infected with PEDV, SADS-CoV, or PDCoV at 100 50% tissue culture infective dose ($TCID_{50}$), respectively. Untransfected Vero-81 or LLC-PK1 cells were infected by these viruses and served as a mock infection control. At 36 hours post-infection (h.p.i.), cell transfection efficiency and cytopathic effect (CPE) images were captured under an inverted fluorescence/phase-contrast microscopy (ZEISS, Germany).

Immunofluorescence staining

Immunofluorescence assays were performed to detect PEDV, SADS-CoV, and PDCoV in the established stable Vero-81 or LLC-PK1 cell lines with multi-shRNA and shRNA-NC expression as previously described (Li et al., 2018a; Song et al., 2015; Zhou et al., 2018b) using mouse monoclonal antibody against the M protein of PEDV and SADS-CoV, or the N protein of PDCoV prepared in our laboratory. After incubation for 1 h at 37°C, cells were washed with PBS (0.01 M, pH 7.4) three times and incubated with FITC-conjugated goat anti-mouse secondary antibodies (Transgen Biotech, China) for 1 h at 37°C. Cells were then washed with PBS and incubated in 0.1 μg/ml 4', 6-diamidino-2-phenylindole (DAPI) (Sigma, USA) for 5 min. The fluorescent images were captured using fluorescent microscopy.

MTS assay

The established stable cell lines of Vero-81 or LLC-PK1 expressing multi-shRNA and shRNA-NC were seeded into 96-well plates at a density of 1×10^4/well. After reaching 100% confluence, the cells were challenged with PEDV, SADS-CoV, or PDCoV at 100 $TCID_{50}$ per well.

At 24 h.p.i., cells were washed with PBS three times, and then cell viability was assessed by adding 20 μl per well of CellTiter 96 AQueous^{TM} One Solution Cell Proliferation Assay (MTS, Promega, USA) directly into the cell culture media. The cells were incubated for 4 h with MTS reagent, and the light absorbance at 490 nm was measured. Percent cell viability (%) was calculated using the mean OD value of the treated cells relative to that of the mock infection control. The experiment performed utilizing three technical replicates.

Viral titer assay

PEDV, SADS-CoV, or PDCoV infected Vero-81 or LLC-PK1 cells with multi-shRNA and shRNA-NC expression and supernatants were collected at 48 h.p.i. After three freeze-thaw cycles and clarification by centrifugation at 4,000 × g for 15 min at 4°C, the viral titer was measured using standard $TCID_{50}$ assay. The cultures were serially diluted tenfold from 10^{-1} to 10^{-10}, and added onto a monolayer of Vero-81 cells or LLC-PK1 cells in 96-well culture plates. Each dilution was added to eight wells. After 3 days of infection, CPE was assessed microscopically and $TCID_{50}$ was calculated by the Reed-Muench method (Li et al., 2011).

Quantitative real-time PCR

The established stable cell lines of Vero-81 or LLC-PK1 expressing multi-shRNA and shRNA-NC were harvested at 48 h.p.i. and total RNA was extracted using MiniBEST^{TM} Universal RNA Extraction Kit (Takara, China). The mRNA levels of the targeting genes (the M gene of PEDV and SADS-CoV, and the N gene of PDCoV) and non-targeting genes (the ORF1 and S genes of PEDV, SADS-CoV, and PDCoV) were determined by quantitative real-time PCR (qPCR) using the one Step SYBR PrimeScript^{TM} PLUS RT-PCR Kit (Takara, China) and the gene-specific primers described previously are presented in Supplementary Table 2 (Li et al., 2018a; Song et al.,

2015; Zhou et al., 2018a; Zhou et al., 2010). PCR amplification was carried out using an ABI 7500 Real-Time PCR System (Thermo Fisher, USA) under the following conditions: initial denaturation at 95°C for 30 s, and then 40 cycles of 95°C for 5 s and 61°C for 30 s; the melting curve stage comprised 95°C for 1 min, 55°C for 30 s, and 95°C for 30 s. The relative amounts of viral RNAs in each sample were normalized to the expression of *β*-actin as an internal control by $2^{-\triangle\triangle Ct}$ method (Shen et al., 2015). All experiments were repeated three times.

Western blot

At 48 h.p.i., total proteins were extracted from cells and western blots were performed as reported previously (Fang et al., 2017; Li et al., 2015; Zhou et al., 2018b) using primary antibodies against PEDV, SADS-CoV, and PDCoV as described in the "Immunofluorescence staining" section above and a mouse polyclonal anti-*β*-actin for loading control (Transgen, China). Equal amount of each sample was heated at 70°C for 10 min, separated in 12% sodium dodecyl sulfate-polyacrylamide gel electrophoresis (SDS-PAGE), then electrotransfered to polyvinylidene difluoride membranes. The membranes were incubated with primary antibodies at 4°C overnight, washed three time with PBS plus 0.05% Tween-20, and incubated with horseradish peroxidase-conjugated anti-mouse IgG at 37°C for 1 h. Proteins were detected by adding electrochemiluminescence substrate (GenScript, USA). Image analysis was performed with Image Lab software (Biorad, USA).

Statistical analysis

Statistical analysis of the data from qPCR and MTS assays were performed using GraphPad Prism Software version 5.01 (GraphPad Software, USA). Significant differences were determined by Student's *t* test. A p-value of < 0.05 (*) was considered significantly different and a p-value of

< 0.001 (***) was considered highly significant. Data were presented as mean ± standard deviation (SD).

RESULTS

Sequence-specific protection of Vero-81 cells and LLC-PK1 cells from PEDV, SADS-CoV, or PDCoV-induced CPE by multiply-expressed shRNAs

To investigate whether multi-shRNA could protect Vero-81 cells or LLC-PK1 cells from CPE induced by PEDV, SADS-CoV, and PDCoV, pMulti-shRNA-M/N-mCherry-transfected cells were infected and assessed. pSil-shRNA-NC-mCherry was used as nonspecific transfection control. At 36 h.p.i. with 100 $TCID_{50}$ of PEDV, SADS-CoV, or PDCoV, analysis of CPE indicated that Vero-81 or LLC-PK1 cells in the mock or negative transfection controls became reticulated and detached from the monolayer. However, CPE was rarely observed in SECoV-infected Vero-81 or LLC-PK1 cells expressing specific multi-shRNA. Control staining for shRNA vector (mCherry), viral protein (FITC), and cell monolayer (DAPI) indicated that CPE was directly associated with loss of cell monolayer with viral replication (Figures 1-3).

Increased viability of PEDV, SADS-CoV, and PDCoV infected cells induced by multiple-shRNA

To further study the effect of multi-shRNA on protecting cells against PEDV, SADS-CoV, or PDCoV infection, cell viability determined by a MTS assay was performed. Since there is a linear response between cell number and the absorbance readout, the absorbance value at 490 nm is directly proportional to the number of living cells in culture (Supplementary Figure 2). Compared with nonspecific transfection (pSil-shRNA-NC-mCherry) control and mock (nontransfected

plasmind) transfection control cells, specific transfection (pMulti-shRNA-M/N-mCherry) cells were highly effective in inhibiting SECoV-induced CPE at 28 h.p.i. This phenomenon indicated that the multi-shRNA-expressing plasmid could significantly protect cells from PEDV infection. The viability (mean ± SD %) of multi-shRNA-expressing cells was 95.13 ± 1.49% (Figure 4a), which was obviously higher ($p < 0.001$) than that of the nonspecific transfection control (49.67 ± 0.43%) and the mock transfection control (44.90 ± 0.37%). Likewise, in Vero-81 cells infected with SADS-CoV at 28 h.p.i., these similar results were observed, indicating that the multi-shRNA-expressing plasmid could prevent cells from SADS-CoV infection. The cell viability of pMulti-shRNA-M/N-mCherry transfected cells was 97.45 ± 1.06 % (Figure 4b), which was far greater ($p < 0.001$) than that of the nonspecific transfection control (24.00 ± 0.33%) and the mock transfection control (24.82 ± 0.54%). As expected, the similar situation in LLC-PK1 cells infected with PDCoV were observed compared to the experimental data from Vero-81 cells. It was suggested the multi-shRNA-expressing plasmid could sufficiently protect cells from PDCoV infection. In addition, the viability of cells expressing multi-shRNA was 92.87 ± 1.6 % (Figure 4c), which was considerably higher ($p < 0.001$) than that of the nonspecific transfection control (58.03 ± 1.39 %) and the mock transfection control (50.66 ± 3.31 %). Taken together, our results indicated that multi-shRNA-treated cell conditions maintained a level of cell viability comparable to those of uninfected controls, while SECoV-infected nonspecific-shRNA-treated cells experienced a loss of viability comparable to infected cells lacking specific shRNA expression.

Multiple-shRNA-mediated reduction in production of infectious virus

To substantiate the inhibitory effect of shRNAs on production of viable virus, $TCID_{50}$ was used to titrate PEDV, SADS-CoV, and PDCoV at 48 h.p.i. PEDV results showed that in nonspecific-transfected control cells, virus titer reached $10^{6.04 \pm 0.07}$ $TCID_{50}$/ml, which was similar to that observed in mock transfected control cells ($10^{6.61 \pm 0.14}$ $TCID_{50}$/ml). In contrast, the titer determined in cells transfected with pMulti-shRNA-M/N-mCherry was $10^{3.21 \pm 0.11}$ $TCID_{50}$/ml (Figure 5a), which was reduced by 2500-fold ($p < 0.001$) compared to that of PEDV in mock transfected control cells. SADS-CoV data showed that the virus titers of nonspecific transfection and mock transfection controls were $10^{5.63 \pm 0.05}$ $TCID_{50}$/ml and $10^{5.71 \pm 0.09}$ $TCID_{50}$/ml, respectively. Conversely, the titer in cells transfected with pMulti-shRNA-M/N-mCherry was only $10^{2.38 \pm 0.04}$ $TCID_{50}$/ml (Figure 5b) and reduced by 2100-fold ($p < 0.001$) compared to that of SADS-CoV in mock transfected control cells. PDCoV data demonstrated the virus titers in nonspecific transfection and mock transfection controls were as high as $10^{8.23 \pm 0.06}$ $TCID_{50}$/ml and $10^{8.53 \pm 0.08}$ $TCID_{50}$/ml, respectively. In contrast, the titer in multi-shRNA-expressing cells was $10^{4.13 \pm 0.07}$ $TCID_{50}$/ml (Figure 5c), which resulted in up to 25000-fold ($p < 0.001$) drop compared to that of PDCoV in mock transfected control cells. These data indicated that pMulti-shRNA-M/N-mCherry could significantly inhibit the complete replication *in vitro* of infectious PEDV, SADS-CoV, and PDCoV.

Multiple-shRNA-mediated inhibition of viral RNA replication

To assess the influence of multi-shRNA expression on SECoVs genomic RNA replication, the M gene of PEDV and SADS-CoV, and the N gene of PDCoV (these targeting genes of multi-shRNA expression system) were used, respectively, as proxies. A real-time RT-PCR quantitative analysis of mRNA expression level of M or N was normalized to the corresponding

β-actin in the same sample. The relative amounts of M or N gene in SECoV-infected transfected control cells were regarded as 1.000 (Shen et al., 2015). In PEDV, the relative expression levels of the M gene in multi-shRNA or shRNA-NC expressing cells were 0.003 ± 0.001 or 0.887 ± 0.003, respectively. These data indicated that PEDV genome RNA in specific-transfected cells were reduced by 99.7 %, compared to those of the mock transfection control ($p<0.001$) (Figure 6a). There is a similar situation in SADS-CoV infection. The relative amounts of the M gene in cells transfected with pMulti-shRNA-M/N-mCherry and pSil-shRNA-NC-mCherry were 0.006 ± 0.001 and 0.977 ± 0.002, which indicated SADS-CoV genome RNA in multi-shRNA expressing cells were dropped by 99.4 %, compared to those of the non-transfection control ($p <0.001$) (Figure 6b). The relative amounts of the N gene in PDCoV-infected cells containing pMulti-shRNA-M/N-mCherry and pSil-shRNA-NC-mCherry were 0.012 ± 0.001 and 0.963 ± 0.004. Compared to those of the negative transfection control, the specific-transfected group showed that the amounts of PDCoV genome RNA in cells expressing multi-shRNA were reduced by 98.8 % ($p <0.001$) (Figure 6c). The mRNA expression levels of the ORF1 and S genes, non-targeting genes of multi-shRNA expression system, of SECoVs were tested by qPCR as well, and the results were consistent with those of the targeting genes (Supplementary Figure 3). Overall, these data suggested a potent inhibition of PEDV, SADS-CoV, and PDCoV genome RNA replication triggered by sequence-specific multi-shRNA in Vero-81 cells or LLC-PK1 cells.

Detection of the levels of viral proteins by western blot

To further investigate the effect of multi-shRNA on protein synthesis of PEDV, SADS-CoV, and PDCoV, the expression levels of viral proteins at 48 h.p.i. were examined using western blot. Figure 7 shows that the amounts of viral proteins including PEDV N protein, SADS-CoV M

protein, and PDCoV N protein harvested from the multi-shRNA expressing cells were dramatically reduced, which was consistent with the qPCR analysis (Figure 6 and Supplementary Figure 3) and with reduced viral protein staining in cultures expressing multi-shRNA (Figure 1-3).

DISCUSSION

SECoVs, which lead to substantial economic losses, are the major concern in swine severe diarrhea diseases since there currently are no effective treatments. RNAi technology might represent a potential strategy for the control of these diseases. Successful RNAi on the inhibition of PEDV replication has been demonstrated by synthetic siRNA and plasmid-transcribed shRNA targeting M gene (Shen et al., 2015). However, recent epidemiological studies revealed that the presence of multiple virus strains simultaneously circulated in many endemic areas including PEDV, SADS-CoV, and PDCoV (Ajayi et al., 2018; Niederwerder and Hesse, 2018; Trudeau et al., 2017; Zhou et al., 2018b). Both PEDV and SADS-CoV are classified into group of the genus *Alphacoroavirus*, and their membrane gene share highly similar nucleotide structure. The M protein of coronavirus not only plays a vital role in the viral assembly, but also can neutralize anti-M antibody under the existence of complement (Raaben et al., 2009). Meanwhile, the N protein forms complexes with genomic RNA of coronavirus and enhances the process of virus transcription and assembly. The N protein is the predominant antigen produced in infected cells, which makes it a major target for the accurate and early diagnosis (Kuo et al., 2016). Therefore, it is essential to design a dual-shRNA system that expresses multiple shRNAs to block a variety of SECoVs simultaneously.

For the development of a durable gene therapy that prevents infection from a range of SECoVs, an expression vector was designed to simultaneously express multiple shRNAs targeting the M protein gene of PEDV and SADS-CoV, and the N protein gene of PDCoV. The shRNA expression cassettes in this vector were designed with a *Bam*H□ restriction site compatible with *Bgl*□ and allowing combination of two or more shRNAs expression cassettes in a building block manner. An analogous cloning strategy has been independently applied in the construction of a vector that was intended to silence two endogenously expressed genes simultaneously. The advantages of multi-shRNA expression vector is exhibited using a model system simulating the emergence of mutated viruses (Ma et al., 2014). This approach also could provide a possible therapeutic option against multiple-virus co-infections.

In order to express multiple shRNAs, we utilize a dual promoter system containing two copies of the hU6 promoter, an RNA Pol □ promoter. Pol □ promoters have been widely used to mediate the high-level expression of shRNAs. However, shRNA expression driven by RNA Pol □ promoters has been shown to induce cell toxicity and lethality in adult mice (Giering et al., 2008). While cell toxicity potentially associated with two hU6 promoters was a concern in this study, no significant cytotoxic effects were observed in Vero-81 or LLC-PK1 cells. Our results were consistent with the previous study of adenovirus vector expressing two shRNAs under control of two hU6 promoters, which did not show any obvious cytotoxicity in IBRS-2 cells (Kim et al., 2008). In contrast, the adenovirus with three separate hU6 promoters has some cytotoxic effects (Chen and Mahato, 2008). The increased toxicity might be associated with the interference of the cellular RNAi pathway induced Pol □ promoter (Giering et al., 2008). Therefore, to ensure efficient inhibition of viral replication *in vitro*, we constructed that the multi-shRNA expression

plasmid flanked two independent hU6 promoters to minimize the cytotoxicity potentially caused by excessive RNA Pol □ promoter. In this report, the multi-shRNA expression system can inhibit virus replication without significant cytotoxicity *in vitro*. When the multi-shRNA expression vector was employed against the PEDV, SADS-CoV, and PDCoV simultaneously, it was found to silence the target gene with high potency, comparable to that of the individual single-shRNA expression vector (Shen et al., 2015; Zhou et al., 2010). This phenomenon also was observed in the experiment data from corresponding study on simultaneous expression of multiple shRNAs for the target genes of HIV and HBV, which had antiviral effects against both these viruses, showing a significant efficiency compared with that of separate applications of each single shRNA (Wu et al., 2007).

In conclusion, we introduced a novel multiple-resistance strategy against three major harmful viral diarrhea diseases in neonatal pigs. Notably, this work represents a significant advance, potentially facilitating new experimental approaches for the analysis of both viral and cellular gene functions in the context of infection with multiple infections with SECoVs. Taken together, our data show that the tremendous potential for this multiple-shRNA expression vector is enable to precisely and effectively interfere with the replication of multiple SECoVs *in vitro*.

Acknowledgements

This work was supported by the National Key Research and Development Program [grant number 2017YFD0500600], the Natural Science Foundation of Jiangxi Province [grant number 2018ACB21027 and 20161BAB214169], the Graduate Research & Innovation Projects in Jiangxi

Province [grant number YC2017-B036], and Science and Technology Project of Education Department of Jiangxi Province [grant number GJJ150388].

Declarations of interest: none

Figure Legends

Figure 1. Effect of multi-shRNA on PEDV-induced CPE in Vero-81 cells by immunofluorescence assay. (a–d) pMulti-shRNA-M/N-mCherry transfected cells showed remarkable reduction of viral protein expression; (e–h) Non-transfected cells with infection were used as mock transfection control; (i–l) pSil-shRNA-NC-mCherry transfected cells showed no detectable effect on virus infection as nonspecific transfection control; (m–p) Non-transfected and non-infected cells were used as untreated blank control. The bright green color indicated the presence of viral protein-positive cells. The cherry red color indicated the presence of the transfected cells. The nuclei were stained blue by DAPI (×100 magnification).

Figure 2. Effect of multi-shRNA on SADS-CoV-induced CPE in Vero-81 cells by immunofluorescence assay. Treatments of cells and illustrations were the same as those described in legend to Figure 1.

Figure 3. Effect of multi-shRNA on PDCoV-induced CPE in LLC-PK1 cells by immunofluorescence assay. Treatments of cells and illustrations were the same as those described in legend to Figure 1.

Figure 4. The Vero-81 cells or LLC-PK1 cells viability was calculated using the MTS assay at 28 h.p.i. (a) PEDV infected group, (b) SADS-CoV infected group, (c) PDCoV infected group.

Figure 5. Reduction in titers of PEDV (a), SADS-CoV (b), and PDCoV (c) in Vero-81 cells or LLC-PK1 cells expressing multi-shRNA.

Figure 6. Inhibition of PEDV, SADS-CoV, and PDCoV RNA replication by multi-shRNA in Vero-81 cells or LLC-PK1 cells. Quantitative real-time PCR detection of PEDV M gene (a) , SADS-CoV M gene (b), and PDCoV N gene (c) mRNA transcripts relative to β-actin transcripts in the same sample.

Figure 7. Expression of viral proteins of PEDV (a), SADS-CoV (b), and (c) PDCoV assessed by western blot. Equal amounts of cell lysates at 48 h.p.i. were examined using monoclonal antibodies against N protein of PEDV, M protein of SADS-CoV, or N protein of PDCoV, with β-actin as a protein loading control.

Table 1. The inserted sequences in shRNA-expressing plasmids

Name	Sequence[a]
Bgl□-PEDV/SADS-M-*Ec* *o*R□-F:	5’-gatcGCTGGAATWTCAYAYGGAATttcaagagaATTCCRTRTGAWATTCCAGTTTTTTg-3’
Bgl□-PEDV/SADS-M-*Ec* *o*R□-R:	5’-aattcAAAAAACTGGAATWTCAYAYGGAATtctcttgaaATTCCRTRTGAWATTCCAGC-3’
Xho□-PDCoV-N-*Kpn*□-F:	5’-tcgagGGCTGACACTTCTATTAAAttcaagagaTTTAATAGAAGTGTCAGCCTTTTTTggtac-3’
Xho□-PDCoV-N-*Kpn*□-R:	5’-cAAAAAAGGCTGACACTTCTATTAAAtctcttgaaTTTAATAGAAGTGTCAGCCc-3’
Bgl□-NC-*Eco*R□-F:	5’-gatcGCTAGTATGTGCGTGCGGTTttcaagagaAACCGCACGCACATACTAGTTTTTTg-3’
Bgl□-NC-*Eco*R*I*-R:	5’-aattcAAAAAACTAGTATGTGCGTGCGGTTtctcttgaaAACCGCACGCACATACTAGC-3’
Xho□-NC-*Kpn*□-F:	5’-tcgagCTAGTATGTGCGTGCGGTTttcaagagaAACCGCACGCACATACTAGTTTTTTggtac-3’
Xho□-NC-*Kpn*□-R:	5’-cAAAAAACTAGTATGTGCGTGCGGTTtctcttgaaAACCGCACGCACATACTAGc-3’

[a] Lowercase letters indicated the end sequences of the enzyme digestion reaction; Underlined lowercase letters indicated the loop sequences; Uppercase letters indicated the siRNA sequences. W: A or T; Y: C or T; R: A or G.

Supplementary materials

Supplementary Figure 1. Schematic representation of the construction of multi-shRNA expression vector.

Supplementary Figure 2. The mean OD values of Vero-81 cells or LLC-PK1 cells expressing multi-shRNA after infection by PEDV, SADS-CoV, or PDCoV at 100 $TCID_{50}$. At 28 h.p.i., viable cell numbers were evaluated by MTS assay. (a) PEDV infected group, (b) SADS-CoV infected group, (c) PDCoV infected group.

Supplementary Figure 3. Quantitative real-time PCR detection of the ORF1 gene (a-c) and the S gene (d-f) mRNA transcripts of PEDV, SADS-CoV, and PDCoV relative to β-actin transcripts in the same sample.

Supplementary Table 1. List of siRNA sequences in this study.

Supplementary Table 2. Primers used for quantitative real-time PCR.

REFERENCES

Ajayi, T., Dara, R., Misener, M., Pasma, T., Moser, L., Poljak, Z., 2018. Herd-level prevalence and incidence of porcine epidemic diarrhoea virus (PEDV) and porcine deltacoronavirus (PDCoV) in swine herds in Ontario, Canada. Transboundary and emerging diseases 65, 1197-1207. https://doi.org/10.1111/tbed.12858.

Berkhout, B., 2018. RNAi-mediated antiviral immunity in mammals. Current opinion in virology 32, 9-14. https://doi.org/10.1016/j.coviro.2018.07.008.

Bevins, S.N., Lutman, M., Pedersen, K., Barrett, N., Gidlewski, T., Deliberto, T.J., Franklin, A.B., 2018. Spillover of Swine Coronaviruses, United States. Emerging infectious diseases 24, 1390-1392. https://doi.org/10.3201/eid2407.172077.

Chen, Y., Mahato, R.I., 2008. siRNA pool targeting different sites of human hepatitis B surface antigen efficiently inhibits HBV infection. Journal of drug targeting 16, 140-148. https://doi.org/10.1080/10611860701878750.

Dong, N., Fang, L., Yang, H., Liu, H., Du, T., Fang, P., Wang, D., Chen, H., Xiao, S., 2016. Isolation, genomic characterization, and pathogenicity of a Chinese porcine deltacoronavirus strain CHN-HN-2014. Veterinary microbiology 196, 98-106. https://doi.org/10.1016/j.vetmic.2016.10.022.

Fang, P., Fang, L., Hong, Y., Liu, X., Dong, N., Ma, P., Bi, J., Wang, D., Xiao, S., 2017. Discovery of a novel accessory protein NS7a encoded by porcine deltacoronavirus. The Journal of general virology 98, 173-178. https://doi.org/10.1099/jgv.0.000690.

Fu, X., Fang, B., Liu, Y., Cai, M., Jun, J., Ma, J., Bu, D., Wang, L., Zhou, P., Wang, H., Zhang, G., 2018. Newly emerged porcine enteric alphacoronavirus in southern China: Identification, origin and evolutionary history analysis. Infection, genetics and evolution : journal of molecular epidemiology and evolutionary genetics in infectious diseases 62, 179-187. https://doi.org/10.1016/j.meegid.2018.04.031.

Giering, J.C., Grimm, D., Storm, T.A., Kay, M.A., 2008. Expression of shRNA from a tissue-specific pol II promoter is an effective and safe RNAi therapeutic. Molecular therapy : the journal of the American Society of Gene Therapy 16, 1630-1636. https://doi.org/10.1038/mt.2008.144.

Gong, L., Li, J., Zhou, Q., Xu, Z., Chen, L., Zhang, Y., Xue, C., Wen, Z., Cao, Y., 2017. A New Bat-HKU2-like Coronavirus in Swine, China, 2017. Emerging infectious diseases 23. https://doi.org/10.3201/eid2309.170915.

Guo, J., Fang, L., Ye, X., Chen, J., Xu, S., Zhu, X., Miao, Y., Wang, D., Xiao, S., 2018. Evolutionary and genotypic analyses of global porcine epidemic diarrhea virus strains. Transboundary and emerging diseases. https://doi.org/10.1111/tbed.12991.

Hu, H., Jung, K., Vlasova, A.N., Chepngeno, J., Lu, Z., Wang, Q., Saif, L.J., 2015. Isolation and characterization of porcine deltacoronavirus from pigs with diarrhea in the United States. Journal of clinical microbiology 53, 1537-1548. https://doi.org/10.1128/JCM.00031-15.

Kim, S.M., Lee, K.N., Park, J.Y., Ko, Y.J., Joo, Y.S., Kim, H.S., Park, J.H., 2008. Therapeutic application of RNA interference against foot-and-mouth disease virus in vitro and in vivo. Antiviral research 80, 178-184. https://doi.org/10.1016/j.antiviral.2008.06.001.

Kuo, L., Hurst-Hess, K.R., Koetzner, C.A., Masters, P.S., 2016. Analyses of Coronavirus Assembly Interactions with Interspecies Membrane and Nucleocapsid Protein Chimeras. Journal of virology 90, 4357-4368. https://doi.org/10.1128/JVI.03212-15.

Lau, T.S., Li, Y., Kameoka, M., Ng, T.B., Wan, D.C., 2007. Suppression of HIV replication using RNA interference against HIV-1 integrase. FEBS letters 581, 3253-3259. https://doi.org/10.1016/j.febslet.2007.06.011.

Lee, S.H., Yang, D.K., Kim, H.H., Cho, I.S., 2018. Efficacy of inactivated variant porcine epidemic diarrhea virus vaccines in growing pigs. Clinical and experimental vaccine research 7, 61-69. https://doi.org/10.7774/cevr.2018.7.1.61.

Li, B.J., Tang, Q., Cheng, D., Qin, C., Xie, F.Y., Wei, Q., Xu, J., Liu, Y., Zheng, B.J., Woodle, M.C., Zhong, N., Lu, P.Y., 2005. Using siRNA in prophylactic and therapeutic regimens against SARS coronavirus in Rhesus macaque. Nature medicine 11, 944-951. https://doi.org/10.1038/nm1280.

Li, J., Dai, Y., Liu, S., Guo, H., Wang, T., Ouyang, H., Tu, C., 2011. In vitro inhibition of CSFV replication by multiple siRNA expression. Antiviral research 91, 209-216. https://doi.org/10.1016/j.antiviral.2011.06.005.

Li, K., Song, D., Zhang, F., Gong, W., Guo, N., Li, A., Zhou, X., Huang, D., Ye, Y., Tang, Y., 2018a. Complete Genome Sequence of a Recombinant Porcine Epidemic Diarrhea Virus Strain, CH/JXJA/2017, Isolated in Jiangxi, China, in 2017. Genome announcements 6. https://doi.org/10.1128/genomeA.01590-17.

Li, Q., Xu, Z., Wu, T., Peng, O., Huang, L., Zhang, Y., Xue, C., Wen, Z., Zhou, Q., Cao, Y., 2018b. A flagellin-adjuvanted PED subunit vaccine improved protective efficiency against PEDV variant challenge in pigs. Vaccine 36, 4228-4235. https://doi.org/10.1016/j.vaccine.2018.05.124.

Li, W., Li, H., Liu, Y., Pan, Y., Deng, F., Song, Y., Tang, X., He, Q., 2012. New variants of porcine epidemic diarrhea virus, China, 2011. Emerging infectious diseases 18, 1350-1353. 10.3201/eid1808.120002

Li, Y., Wang, G., Wang, J., Man, K., Yang, Q., 2017. Cell attenuated porcine epidemic diarrhea virus strain Zhejiang08 provides effective immune protection attributed to dendritic cell stimulation. Vaccine 35, 7033-7041. https://doi.org/10.1016/j.vaccine.2017.10.052.

Li, Y., Zheng, F., Fan, B., Muhammad, H.M., Zou, Y., Jiang, P., 2015. Development of an indirect ELISA based on a truncated S protein of the porcine epidemic diarrhea virus. Canadian journal of microbiology 61, 811-817. https://doi.org/10.1139/cjm-2015-0213.

Ma, J., Zeng, L., Fan, Y., Zhou, Y., Jiang, N., Chen, Q., 2014. Significant inhibition of two different genotypes of grass carp reovirus in vitro using multiple shRNAs expression vectors. Virus research 189, 47-55. https://doi.org/10.1016/j.virusres.2014.05.009.

Ma, Y., Zhang, Y., Liang, X., Lou, F., Oglesbee, M., Krakowka, S., Li, J., 2015. Origin, evolution, and virulence of porcine deltacoronaviruses in the United States. mBio 6, e00064. https://doi.org/10.1128/mBio.00064-15.

Mason, P.W., Grubman, M.J., Baxt, B., 2003. Molecular basis of pathogenesis of FMDV. Virus research 91, 9-32.

Niederwerder, M.C., Hesse, R.A., 2018. Swine enteric coronavirus disease: A review of 4 years with porcine epidemic diarrhoea virus and porcine deltacoronavirus in the United States and Canada. Transboundary and emerging diseases 65, 660-675. https://doi.org/10.1111/tbed.12823.

Oh, J.N., Choi, K.H., Lee, C.K., 2018. Multi-resistance strategy for viral diseases and in vitro short hairpin RNA verification method in pigs. Asian-Australasian journal of animal sciences 31, 489-498. https://doi.org/10.5713/ajas.17.0749.

Pan, Y., Tian, X., Qin, P., Wang, B., Zhao, P., Yang, Y.L., Wang, L., Wang, D., Song, Y., Zhang, X., Huang, Y.W., 2017. Discovery of a novel swine enteric alphacoronavirus (SeACoV) in southern China. Veterinary microbiology 211, 15-21. https://doi.org/10.1016/j.vetmic.2017.09.020.

Park, J.E., Shin, H.J., 2018. Porcine epidemic diarrhea vaccine efficacy evaluation by vaccination timing and frequencies. Vaccine 36, 2760-2763. https://doi.org/10.1016/j.vetmic.2018.05.012.

Pulloor, N.K., Nair, S., McCaffrey, K., Kostic, A.D., Bist, P., Weaver, J.D., Riley, A.M., Tyagi, R., Uchil, P.D., York, J.D., Snyder, S.H., Garcia-Sastre, A., Potter, B.V., Lin, R., Shears, S.B., Xavier, R.J., Krishnan, M.N., 2014. Human genome-wide RNAi screen identifies an essential role for inositol pyrophosphates in Type-I interferon response. PLoS pathogens 10, e1003981. https://doi.org/10.1371/journal.ppat.1003981.

Raaben, M., Groot Koerkamp, M.J., Rottier, P.J., de Haan, C.A., 2009. Type I interferon receptor-independent and -dependent host transcriptional responses to mouse hepatitis coronavirus infection in vivo. BMC genomics 10, 350. https://doi.org/10.1186/1471-2164-10-350

Shen, H., Zhang, C., Guo, P., Liu, Z., Zhang, J., 2015. Effective inhibition of porcine epidemic diarrhea virus by RNA interference in vitro. Virus genes 51, 252-259. https://doi.org/10.1007/s11262-015-1242-5.

Song, D., Zhou, X., Peng, Q., Chen, Y., Zhang, F., Huang, T., Zhang, T., Li, A., Huang, D., Wu, Q., He, H., Tang, Y., 2015. Newly Emerged Porcine Deltacoronavirus Associated With Diarrhoea in Swine in China: Identification, Prevalence and Full-Length Genome Sequence Analysis. Transboundary and emerging diseases 62, 575-580. https://doi.org/10.1111/tbed.12399.

Stadejek, T., Stankevicius, A., Murtaugh, M.P., Oleksiewicz, M.B., 2013. Molecular evolution of PRRSV in Europe: current state of play. Veterinary microbiology 165, 21-28. https://doi.org/10.1016/j.vetmic.2013.02.029.

Su, Y., Hou, Y., Prarat, M., Zhang, Y., Wang, Q., 2018. New variants of porcine epidemic diarrhea virus with large deletions in the spike protein, identified in the United States, 2016-2017. Archives of virology 163, 2485-2489. https://doi.org/10.1007/s00705-018-3874-y.

Sui, H.Y., Zhao, G.Y., Huang, J.D., Jin, D.Y., Yuen, K.Y., Zheng, B.J., 2009. Small interfering RNA targeting m2 gene induces effective and long term inhibition of influenza A virus replication. PloS one 4, e5671. https://doi.org/10.1371/journal.pone.0005671.

Trudeau, M.P., Verma, H., Sampedro, F., Urriola, P.E., Shurson, G.C., Goyal, S.M., 2017. Environmental persistence of porcine coronaviruses in feed and feed ingredients. PloS one 12, e0178094. https://doi.org/10.1371/journal.pone.0178094.

Wang, H., Cong, F., Zeng, F., Lian, Y., Liu, X., Luo, M., Guo, P., Ma, J., 2018a. Development of a real time reverse transcription loop-mediated isothermal amplification method (RT-LAMP) for detection of a novel swine acute diarrhea syndrome coronavirus (SADS-CoV). Journal of virological methods 260, 45-48. https://doi.org/10.1016/j.jviromet.2018.06.010.

Wang, L., Su, S., Bi, Y., Wong, G., Gao, G.F., 2018b. Bat-Origin Coronaviruses Expand Their Host Range to Pigs. Trends in microbiology 26, 466-470. https://doi.org/10.1016/j.tim.2018.03.001.

Watanabe, T., Hatakeyama, H., Matsuda-Yasui, C., Sato, Y., Sudoh, M., Takagi, A., Hirata, Y., Ohtsuki, T., Arai, M., Inoue, K., Harashima, H., Kohara, M., 2014. In vivo therapeutic potential of Dicer-hunting siRNAs targeting infectious hepatitis C virus. Scientific reports 4, 4750. https://doi.org/10.1038/srep04750.

Wu, K., Mu, Y., Hu, J., Lu, L., Zhang, X., Yang, Y., Li, Y., Liu, F., Song, D., Zhu, Y., Wu, J., 2007. Simultaneously inhibition of HIV and HBV replication through a dual small interfering RNA

expression system. Antiviral research 74, 142-149. https://doi.org/10.1016/j.antiviral.2006.11.004.

Xu, Z., Zhang, Y., Gong, L., Huang, L., Lin, Y., Qin, J., Du, Y., Zhou, Q., Xue, C., Cao, Y., 2018. Isolation and characterization of a highly pathogenic strain of Porcine enteric alphacoronavirus causing watery diarrhoea and high mortality in newborn piglets. Transboundary and emerging diseases. https://doi.org/10.1111/tbed.12992.

Yu, J., Chai, X., Cheng, Y., Xing, G., Liao, A., Du, L., Wang, Y., Lei, J., Gu, J., Zhou, J., 2018. Molecular characteristics of the spike gene of porcine epidemic diarrhoea virus strains in Eastern China in 2016. Virus research 247, 47-54. https://doi.org/10.1016/j.virusres.2018.01.013.

Zhou, J., Huang, F., Hua, X., Cui, L., Zhang, W., Shen, Y., Yan, Y., Chen, P., Ding, D., Mou, J., Chen, Q., Lan, D., Yang, Z., 2010. Inhibition of porcine transmissible gastroenteritis virus (TGEV) replication in mini-pigs by shRNA. Virus research 149, 51-55. https://doi.org/10.1016/j.virusres.2009.12.012.

Zhou, L., Sun, Y., Wu, J.L., Mai, K.J., Chen, G.H., Wu, Z.X., Bai, Y., Li, D., Zhou, Z.H., Cheng, J., Wu, R.T., Zhang, X.B., Ma, J.Y., 2018a. Development of a TaqMan-based real-time RT-PCR assay for the detection of SADS-CoV associated with severe diarrhea disease in pigs. Journal of virological methods 255, 66-70. https://doi.org/10.1016/j.jviromet.2018.02.002.

Zhou, P., Fan, H., Lan, T., Yang, X.L., Shi, W.F., Zhang, W., Zhu, Y., Zhang, Y.W., Xie, Q.M., Mani, S., Zheng, X.S., Li, B., Li, J.M., Guo, H., Pei, G.Q., An, X.P., Chen, J.W., Zhou, L., Mai, K.J., Wu, Z.X., Li, D., Anderson, D.E., Zhang, L.B., Li, S.Y., Mi, Z.Q., He, T.T., Cong, F., Guo, P.J., Huang, R., Luo, Y., Liu, X.L., Chen, J., Huang, Y., Sun, Q., Zhang, X.L., Wang, Y.Y., Xing,

S.Z., Chen, Y.S., Sun, Y., Li, J., Daszak, P., Wang, L.F., Shi, Z.L., Tong, Y.G., Ma, J.Y., 2018b. Fatal swine acute diarrhoea syndrome caused by an HKU2-related coronavirus of bat origin. Nature 556, 255-258. https://doi.org/10.1038/s41586-018-0010-9.

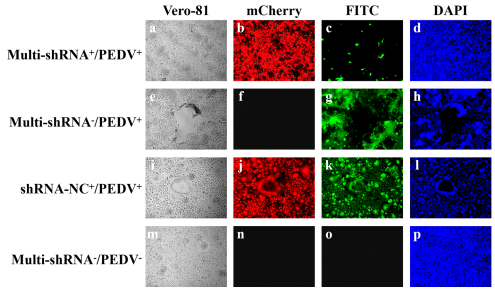

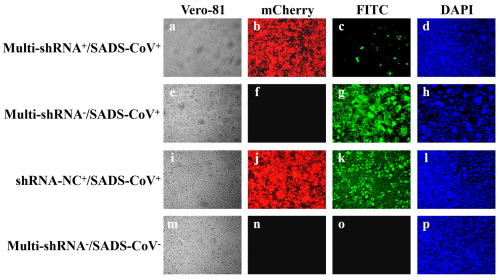

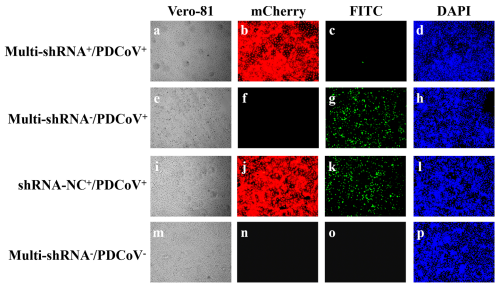

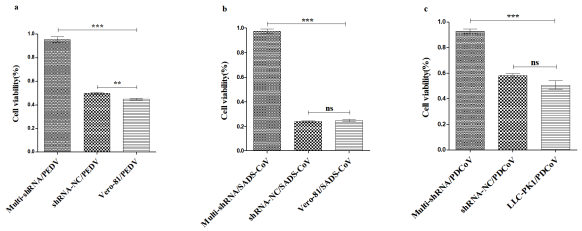

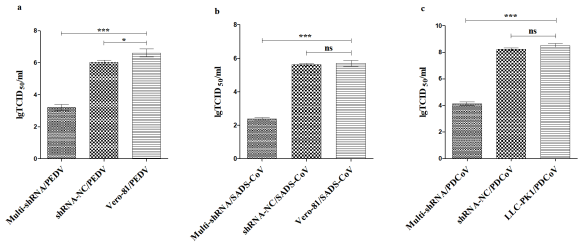

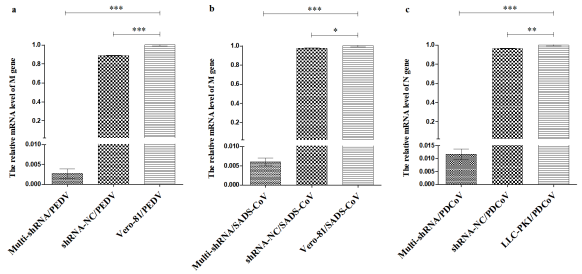

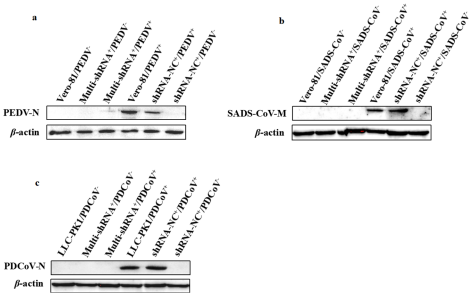

HIGHLIGHT

·Two potential targets of antiviral molecules for the treatment of three swine enteric coronaviruses replication are tested.

·The multiple-shRNA expression vector was constructed to effectively inhibit PEDV, SADS-CoV, and PDCoV.

·A shRNA-based, multiple-resistance antiviral strategy was evaluated *in vitro* and found to significantly affect viral replication.